MECHANICAL INTERACTION BETWEEN SPHERICAL INHOMOGENEITIES: AN ASSESSMENT OF A METHOD BASED ON THE EQUIVALENT INCLUSION

Christophe Fond[1], Arnaud Riccardi[2], Robert Schirrer[1] and Frank Montheillet[2]

[1]Institut Charles Sadron, 6, rue Boussingault F67083 Strasbourg.
fond@ics.u-strasbg.fr tel. (33) 3 88 41 41 68 fax (33) 3 88 41 40 99
schirrer@ics.u-strasbg tel. (33) 3 88 41 41 36 fax (33) 3 88 41 40 99

[2]Ecole Nationale Supérieure des Mines de St Etienne, Centre S.M.S., C.N.R.S. U.R.A. 1884, 158 Cours Fauriel F42023 Saint-Etienne, cedex 2.
montheil@emse.fr tel. : (33) 4 77 42 00 26 fax : (33) 4 77 42 01 57

Abstract: This paper assesses the ability of the Equivalent Inclusion Method (EIM) with third order truncated Taylor series (Moschovidis and Mura, 1975) truncated up to the third order to describe the stress distributions of interacting inhomogeneities. The cases considered are two identical spherical voids and glass or rubber inhomogeneities in an infinite elastic matrix. Results are compared with those obtained using spherical dipolar coordinates, which are assumed to be exact, and by a Finite Element Analysis. The EIM gives better results for voids than for inhomogeneities stiffer than the matrix. In the case of rubber inhomogeneities, while the EIM gives accurate values of the hydrostatic pressure inside the rubber, the stress concentrations are inaccurate at very small neighbouring distances for all stiffnesses. A parameter based on the residual stress discontinuity at the interface is proposed to evaluate the quality of the solution given by the EIM. Finally, for inhomogeneities stiffer than the matrix, the method is found to diverge for expansions in Taylor series truncated at the third order.

Key words: elasticity, interaction, inhomogeneities, equivalent inclusion method, dipolar coordinates

1. INTRODUCTION

Evaluation of the mechanical interactions between inhomogeneities is a problem of interest for several types of material obtained by blending or phase separation. When the role of the second phase is the mechanical stiffening or toughening of the matrix, the volume fraction of inhomogeneities is generally such that the mechanical solutions obtained for a dilute second phase are inaccurate. Moreover, the randomness of the spatial distribution of inhomogeneities can play a key role in the toughening of materials (Fond et al., 1998), which makes impossible any elastic analysis based on a unit cell in a periodic matrix, since the latter introduces order into the morphology.

In the case of polymeric amorphous matrices toughened with spherical rubber inhomogeneities, the hydrostatic pressure in the rubber induces cavitation and hence whitening (Schirrer et al., 1996; Fond et al., 1996). Although these materials exhibit good mechanical properties at medium strain rates, their impact properties have still to be improved (Béguelin, 1996). Fortunately for a mesoscopic analysis, the higher the strain rate, the more realistic is an elastic analysis, to the point where at high strain rates viscosity can be neglected. Owing to the significant increase of the yield stress of the matrix with strain rate, cavitation occurs earlier than plasticity at high strain rates, and a description of the spatial distribution of the cavitated particles requires an analysis of the particle interactions (Géhant, 1999).

In the general case, the complexity of the analysis arises from the morphology, especially in three dimensions, and from the non linear behaviour of the material. If the Finite Element Method (FEM) may be considered as the most powerful tool to analyze the mechanical fields associated with non linear behaviour, it is difficult to correctly mesh a representative volume of the composite material. The Boundary Element Method (BEM) provides an efficient alternative means of taking into account a number of inhomogeneities of arbitrary shape, but again one needs to mesh at least the surfaces in a linear elastic analysis, and also the volumes undergoing plasticity for elastic-plastic materials. Some techniques based on Fourier series can be used to describe a periodic morphology (Suquet, 1990; Moulinec and Suquet, 1998), but it is still necessary to mesh the volume. Thus, as our analysis deals only with spherical inhomogeneities, we chose to use the EIM. The accuracy of the FEM and EIM was evaluated by comparing their approximate solutions to those obtained using spherical dipolar coordinates and the formulation of isotropic elasticity problems (Papkovitch, 1932; Neuber, 1957). Since the latter results could be determined with any desired accuracy, they were considered to be "exact" solutions.

The aim of the present work was to compare various methods of calculating the stress concentrations associated with interacting inhomogeneities and the hydrostatic stresses in rubber inhomogeneities. In rubber toughened polymers, there is a large mechanical contrast between the shear moduli of the matrix and the rubber, typically $\mu^0 / \mu^p = 10^3$, while the ratio of the bulk moduli is typically $K^0 / K^p = 2$. Hence a rubber inhomogeneity behaves practically like a compressible fluid zone (Eshelby, 1957, 1959). This leads to low levels of transmitted tangential stress at the interface and the hydrostatic pressure is then directly related to the volume change of the inhomogeneity. Rubber toughened polymers are known to undergo both damage and plasticity during deformation, the relative importance of the two processes depending on strain rate (Schirrer et al., 1996; Fond et al., 1996). Cavitation generally occurs in the pseudo elastic range of loading and is directly related to the hydrostatic pressure in the rubber, while plasticity and crazing are associated with the stress concentrations.

After justifying the choice of analytical methods, this paper reviews a method based on dipolar coordinates which gives exact solutions, subsequently used as reference solutions. The EIM is then briefly presented and an original "error level indicator" is proposed to estimate the quality of its solutions. In section 5 the accuracy of the method is assessed for two interacting cavities and for two interacting particles stiffer than the matrix. Section 6 presents an analysis of stresses for the particular case of rubber inhomogeneities in a polymer matrix. Finally, in sections 7 and 8 the results are discussed and some conclusions are drawn relating to the EIM.

2. EXACT AXISYMMETRIC SOLUTION FOR TWO INTERACTING SPHERICAL INHOMOGENEITIES

In the formulation of isotropic elasticity problems (Papkovitch, 1932; Neuber, 1944), the axisymmetric displacements are expressed as functions of two harmonic potentials φ and ψ:

$$2\mu\left[u_x, u_y, u_z\right] = grad(\varphi + z\psi) - [0,0,4(1-\nu)\psi] \tag{1}$$

where $\Delta\varphi = \Delta\psi = 0$ and μ and ν are the shear modulus and Poisson ratio in each medium. The above equation is usually written in cartesian coordinates, but here it is more natural to employ spherical dipolar coordinates (α, β, γ) defined by:

$$\begin{cases} x = h(\alpha,\beta)^{-2} \sin\beta\cos\gamma \\ y = h(\alpha,\beta)^{-2} \sin\beta\sin\gamma \\ z = -h(\alpha,\beta)^{-2} \sinh\alpha \end{cases} \tag{2}$$

where $h(\alpha, \beta) = \sqrt{\cosh\alpha - \cos\beta}$ and γ is the angle of revolution. Figure (1) shows the traces of the α = const and β = const surfaces in a meridian plane (γ = const). The spherical interfaces of the two (identical) inhomogeneities correspond to $\alpha = \pm\alpha_1$, the poles P_1 and P_2 are singular points ($\alpha = \pm\infty$) for the spherical dipolar coordinate system, and α and β are equal to zero at infinity.

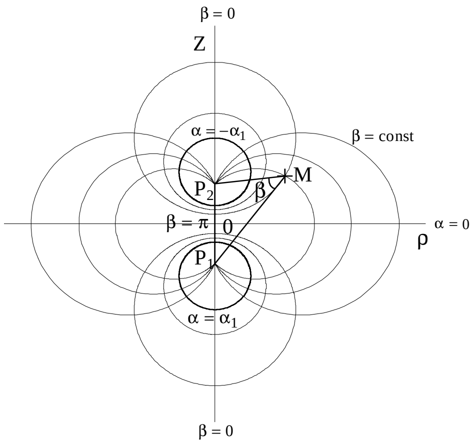

Figure 1. Spherical dipolar coordinate system in a meridian plane $\gamma = const$, with two identical inhomogeneities corresponding to $\alpha = \pm\alpha_1$.

The solution of Laplace's equation in these coordinates is known and the potentials (φ, ψ) may be expressed in terms of Legendre series:

$$\varphi(\alpha,\beta) = h(\alpha,\beta)\sum_{n=0}^{+\infty} A_n\, C_n(\alpha)\, P_n(\cos\beta) \text{ and } \psi(\alpha,\beta) = h(\alpha,\beta)\sum_{n=0}^{+\infty} B_n\, S_n(\alpha)\, P_n(\cos\beta) \tag{3}$$

In the above equations, $P_n(\cos\beta)$ are the polynomial Legendre functions and the unknown coefficients A_n and B_n are associated with the two media (A^i_n, B^i_n for the inclusions and A^m_n, B^m_n for the matrix). $C_n(\alpha) = \cosh(n+1/2)\alpha$ and $e^{-(n+1/2)\alpha}/2$ and $S_n(\alpha) = \sinh(n+1/2)\alpha$ and $-e^{-(n+1/2)\alpha}/2$ within the matrix and inclusions, respectively. Hence the displacements and stress fields associated with the potentials (φ, ψ) and given in spherical dipolar coordinates (Sternberg and Sadowsky, 1952) are valid in the matrix and may also be used in the inclusions by splitting the hyperbolic cosine and sine functions and conserving only the terms involving $e^{-(n+1/2)\alpha}$.

Since the problem is symmetric with respect to the two (identical) inclusions, only the boundary conditions at one of the two inclusion-matrix interfaces, e.g., $\alpha = -\alpha_1$, need be considered. After defining the continuity of displacements and tractions at this interface, assumed to be perfect, using the orthogonality properties of Legendre's polynomials (Sternberg and Sadowsky, 1952), the boundary conditions are transformed into an infinite system of linear equations, which is then truncated and inversed numerically to obtain the unknown coefficients A_n^i, B_n^i and A_n^m, B_n^m.

The truncation order N of the infinite series (3) is determined by the condition that a change from N to N+1 causes a change in the final numerical values of less than the desired error margin and in the present work the convergence of the process was always checked numerically for $N \leq 90$. In order to extend the initial approach of Sternberg and Sadowsky to the case of two interacting spherical inhomogeneities, this method can alternatively be applied to the classical approach of Chen and Acrivos (1978). Although restricted to two inhomogeneities, this would indeed appear to be more convenient, since the use of spherical dipolar coordinates avoids introducing translation operations of the harmonic potentials (φ, ψ).

3. THE EQUIVALENT INCLUSION METHOD

3.1. BRIEF REVIEW OF THE EIM

In the case of inhomogeneities of ellipsoidal shape, analytical solutions are available from the mathematical developments of Ferrers (1877) and Dyson (1891). Using these results and the Eshelby-Kröner static inclusion formalism, Eshelby (1957) found the exact solution for a linear elastic inhomogeneity embedded in an infinite linear elastic matrix and showed that the stress free strain inside the equivalent inclusion is here homogeneous. Sabar et al. (1991) employed the same formalism to take into account a phase transformation or the occurrence of plasticity inside the inclusion in the case of a moving boundary. Wu and Nakagaki (1997) recently proposed an elastoplastic model based on Eshelby's inclusion, where the stress inhomogeneities were assumed to follow a normal distribution. Cherkaoui et al. (1995) also used this formalism for "core and shell" ellipsoids. In linear elastic problems, Moschovidis and Mura (1975) went further than Eshelby (1959) by proposing the use of Taylor series to describe the stress free strain, in order to calculate approximate solutions for interacting inhomogeneities.

Recently, Hort and Johnson (1994) successfully applied the EIM to metallic precipitates having elastic moduli slightly different from those of the matrix. The number of effectively interacting neighbouring spheres was shown to be small and various first order solutions were discussed for the number of neighbouring interacting particles. Rodin and Hwang (1991) proposed a hybrid method coupling the EIM and FEM and involving second order Taylor series, in order to obtain more accurate results than with the EIM for less CPU time. The aim of these authors was to estimate the effective elastic moduli of materials containing spherical inhomogeneities. Due to the nature of the FEM, the simulated materials were partly ordered, being comprised of cubes containing spheres of different radii. The potential energy release given by the EIM was found to be very close to that given by the FEM for two strongly interacting cavities.

The EIM leads to a reduced number of unknowns for inclusion problems, depending on the order of the Taylor series. Thus, once some integrals have been analytically computed for a given geometry of inclusion, the latter may be treated as a three dimensional "element" for which no volume or surface discretization is necessary. This is the fundamental difference as compared to the FEM or the BEM. However, the analytical solution requires efficient computers due to the cumbersome number of terms in the functions, even for relatively low order expansion of the Taylor series. This is one reason why the method has rarely been used for random distributions of inclusions and Taylor series of at least second order. Another reason is that no mathematical proof of the convergence of the EIM has yet been given. In this paper, we propose two dimensionless physically meaningful indicators to evaluate the quality of the solutions and hence test the convergence of the EIM.

Whereas alternative methods are preferable to calculate accurate stress concentration factors for a reduced number of inhomogeneities, typically two (Sternberg and Sadowsky, 1952; Matsuo and Noda, 1997), or for specific problems involving inhomogeneities, for instance the load transfer between rigid spherical inclusions (Phang-Thien and Kim, 1994), the EIM appears to represent a good compromise between accuracy and the spatial distribution of inhomogeneities necessary to describe duplex materials. Many of these materials including rubber toughened polymers contain quasi-spherical inhomogeneities, while for a spherical inclusion the elliptical integrals become analytic functions. Since our present interest was focused on amorphous materials, the EIM was applied to isotropic linear elastic materials and used to obtain approximate solutions involving Taylor series up to the third order.

3.2. EIGENSTRAIN AND STRESS FREE STRAIN

An inclusion is a domain of the matrix which is subjected to a stress free strain, in other words, a thermal dilatation, plastic strain or phase transformation strain which would not induce any stress in the inclusion if it were not embedded in a matrix. An inhomogeneity is a domain with elastic constants different from those of the matrix. Stresses arise from incompatibility of the deformation between the inclusion and the surrounding matrix, assuming perfect adhesion at the inclusion-matrix interface. An eigenstrain is a strain induced by a stress free strain in an inclusion (Mura, 1993).

The EIM has been described in detail elsewhere (Moschovidis and Mura, 1975; Mura, 1993) and only a brief summary will be given below. The present notation differs slightly from that of other papers: bold characters denote tensors and vectors and italics exact functions, while for the sake of clarity, the stress free strain tensors $\mathsf{B}^{\mathbf{p}}$ take values in the pth inclusion and are zero outside. The general equivalence equation is then:

$$\mathbf{C}^{\mathbf{p}}(\mathbf{x})\Big(\boldsymbol{\varepsilon}^{\mathbf{0}}(\mathbf{x}) + \sum_{q=1}^{N} \mathsf{D}^{\mathbf{q}}(\mathbf{x}-\mathrm{x}_{\mathbf{q}})\ \mathsf{B}^{\mathbf{q}}(\mathbf{x})\Big) = \mathbf{C}^{\mathbf{0}}\Big(\boldsymbol{\varepsilon}^{\mathbf{0}}(\mathbf{x}) + \sum_{q=1}^{N} \mathsf{D}^{\mathbf{q}}(\mathbf{x}-\mathrm{x}_{\mathbf{q}})\ \mathsf{B}^{\mathbf{q}} - \mathsf{B}^{\mathbf{p}}(\mathbf{x})\Big) \tag{4}$$

for every point $\mathbf{x} = (x, y, z)$ inside an inhomogeneity (left hand side) or inclusion (right hand side), where N is the number of inclusions and $\mathbf{x}_q = (x_q, y_q, z_q)$ the centre of the qth inclusion. $\mathsf{D}^{\mathbf{p}}$ is a fourth order tensor representing the eigenstrains, which are the effects of $\mathsf{B}^{\mathbf{p}}$ on the strains at point $\mathbf{x}$. $\boldsymbol{\varepsilon}^{\mathbf{0}}(\mathbf{x})$ denotes the remote strain tensor, the strain which would prevail in the absence of an inhomogeneity. $\mathbf{C}^{\mathbf{p}}$ et $\mathbf{C}^{\mathbf{0}}$ are the compliance tensors of the pth inhomogeneity and the matrix, respectively, and for our purposes $\mathbf{C}^{\mathbf{p}}$ is assumed to be uniform in the inhomogeneities.

In order to use analytical solutions, the stress free strain B_j^{p} is approximated by a Taylor series, which for numerical calculations must be truncated to the order T. The subscript j refers to the component of the strain tensor, using the reduced indices ($11 \to 1$, $22 \to 2$, $33 \to 3$, $23 \to 4$, $13 \to 5$, $12 \to 6$). This leads us to define the stress free strain tensors $\boldsymbol{\beta}^{p}(a, b, c)$ as follows:

$$\mathsf{B}_j^{p}(\mathbf{x}) \approx \sum_{a,b,c}^{0 \le a+b+c \le T} \beta_j^{p}(a, b, c)\ (x-x_p)^a\ (y-y_p)^b\ (z-z_p)^c \tag{5}$$

where a, b and c are positive integers or zero such that $0 \le a + b + c \le T$. The remote strain is approximated in the same way by a Taylor series and it should be noted that the remote strain field $\boldsymbol{\varepsilon}^0$ can be non uniform:

$$\overset{0p}{\underset{j}{\varepsilon}}(\mathbf{x}) \approx \sum_{a,\,b,\,c}^{0 \le a+b+c \le T} \overset{0p}{\underset{j}{\varepsilon}}(a, b, c)(x - x_p)^a\ (y - y_p)^b\ (z - z_p)^c \tag{6}$$

The equivalence equation may then be rewritten:

$$\sum_{a',\,b',\,c'}^{0 \le a'+b'+c' \le T} \mathbf{C}^{\mathbf{p}}(\mathbf{x})\Big[\overset{\mathbf{0p}}{\boldsymbol{\varepsilon}}(a, b, c)(\mathbf{x}) + \sum_{q=1}^{N} \overset{\mathbf{q}}{\mathsf{D}}(a', b', c')(\mathbf{x} - \mathbf{x_q})\ \overset{\mathbf{q}}{\boldsymbol{\beta}}(a', b', c')\Big]$$

$$\approx \sum_{a',\,b',\,c'}^{0 \le a'+b'+c' \le T} \mathbf{C^0}\Big[\overset{\mathbf{0p}}{\boldsymbol{\varepsilon}}(a, b, c)(\mathbf{x}) + \sum_{q=1}^{N} \overset{\mathbf{q}}{\mathsf{D}}(a', b', c')(\mathbf{x} - \mathbf{x_q})\ \overset{\mathbf{q}}{\boldsymbol{\beta}}(a', b', c') - \overset{\mathbf{p}}{\boldsymbol{\beta}}(a, b, c)(\mathbf{x})\Big] \tag{7}$$

for all (a, b, c). The tensors $\overset{\mathbf{q}}{\mathsf{D}}(a', b', c')$ are analytically known. For instance, considering a stress free strain $\beta_1(1, 0, 2) = 1$ ($\mathsf{B}_1 = x\,z^2$ and $\mathsf{B}_i = 0$ for $i \neq 1$), where the origin of the coordinates lies at the centre of the spherical inclusion shown in Figure 2(a), the solution can be derived analytically (Ferrers, 18**77;** Dyson, 1891**;** Eshelby, 19**59;** Moschovidis and Mura, 1975). The corresponding deformed shape is shown in Figure 2(b) and the material outside the inclusion is obviously not stress free.

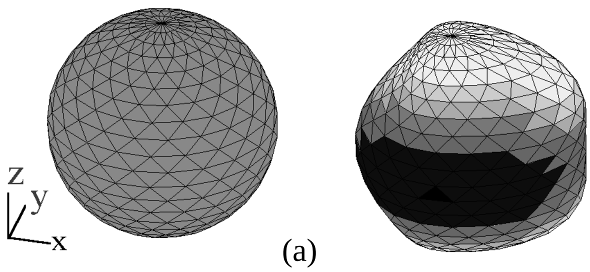

Figure 2. Spherical inclusion (a) subjected to a stress free strain of density xz^2 in a matrix of Poisson's ratio 0.25, and the deformed state (b) (magnification = 5). The level of shading corresponds to the amplitude of the von Mises equivalent stress at the interface.

However, as eq. (7) cannot generally be solved analytically, $\overset{\mathbf{q}}{\mathsf{D}}(a', b', c')$ must also be approximated by a Taylor series in order to obtain a linear system of equations. This leads us to define the fourth order tensor $\overset{pq}{\underset{jk}{D}}(a, b, c, a', b', c')$ as follows:

$$\overset{pq}{\underset{jk}{D}}(a, b, c, a', b', c')\ \overset{q}{\underset{k}{\beta}}(a', b', c') \approx \frac{1}{a!\,b!\,c!}\frac{\partial^a}{\partial x^a}\frac{\partial^b}{\partial y^b}\frac{\partial^c}{\partial z^c}\,\underset{jk}{\mathsf{D}}(\mathbf{x} - \mathbf{x_q})\Big|_{\mathbf{x_p}}\ \overset{q}{\underset{k}{\beta}}(a', b', c') \tag{8}$$

Whereas all strain functions give the exact solution for a single inclusion in an infinite medium, the problem of interacting inhomogeneities leads to approximate solutions because the strains induced by a $\overset{p}{\underset{j}{\beta}}(a, b, c)$ distribution cannot be exactly expressed by a Taylor series with a finite T value at every point. Therefore, the equality between the stress inside an inhomogeneity p and that inside the corresponding equivalent inclusion, which induces an eigenstrain, is rewritten in the form:

$$\sum_{j=1}^{6} C^{p}_{ij} \Big(\varepsilon^{0p}_{j}(a, b, c) + \sum_{k=1}^{6} \sum_{q=1}^{N} \sum_{a', b', c'}^{0 \le a'+b'+c' \le T} D^{pq}_{jk}(a, b, c, a', b', c')\, \beta^{q}_{k}(a', b', c') \Big) =$$

$$\sum_{j=1}^{6} C^{0}_{ij} \Big(\varepsilon^{0p}_{j}(a, b, c) + \sum_{k=1}^{6} \sum_{q=1}^{N} \sum_{a', b', c'}^{0 \le a'+b'+c' \le T} D^{pq}_{jk}(a, b, c, a', b', c')\, \beta^{q}_{k}(a', b', c') - \beta^{p}_{j}(a, b, c) \Big) \tag{9}$$

for all (a, b, c) and for every i and p. The compliance tensors are assumed to be uniform. At this stage, it should be noted that the left hand side of eq. (7), the heterogeneous problem, involves non equilibrated stress fields, while the right hand side, the homogeneous equivalent problem, deals with equilibrated stress fields. The right hand side of this equation is in fact the sum of exact solutions for the inclusion problem. Since $\mathbf{C}^{\mathbf{p}} \neq \mathbf{C}^{\mathbf{0}}$, the left hand side generally involves non equilibrated stress fields due to the normal stress discontinuities at the interface and non zero body forces which remain for truncated Taylor series. Considering now eq. (9), the left hand side concerns non equilibrated stress fields for the same two reasons, while on the right hand side the estimation of $\mathbf{D}$ by truncated Taylor series also mostly leads to non equilibrated stress fields. The exact solution is obtained when the stress field on the left hand side is equilibrated.

If a uniform strain field is applied at infinity, $\varepsilon^{0p}_{j}(a, b, c)$ vanishes whenever $a + b + c \neq 0$. A linear system allowing estimation of the $\beta^{p}_{j}(a, b, c)$, the initial unknowns of the mechanical interaction problem, is obtained by identifying terms of the same order in eq. (9). Since the Taylor series must be truncated, eq. (9) gives an approximate solution, which is expected to increase in quality with inclusion of higher order terms (see section 5). The number of unknowns per inhomogeneity is 6 for a truncation order T of zero, 24 for T = 1, 60 for T = 2, 120 for T = 3, ...

The present evaluation was limited to isotropic materials, where the C_{ij} depend only on the shear and bulk moduli. In the particular case of cavities ($\mu = K = 0$), eq. (9) has no single solution due to the vanishing right hand term and therefore leads to impotent eigenstrains. It is nevertheless possible to derive specific equations for cavities (Mura, 1993). A simple way of avoiding numerical problems without restricting the potential of our software was adopted here: the elastic constants of the cavities were set to 10^{-6} times those of the matrix. Computing with double precision reals makes the error introduced by this simplification negligible compared to that resulting from truncation of the Taylor series.

4. Quality of the solution

The solution given by the equivalence equation (9) is kinetically admissible, accounts for the behaviour of the material and fulfils the boundary conditions, but it is not statically admissible for the following reasons. A polynomial stress free strain of degree N induces a polynomial eigenstrain of the same degree inside an inclusion (Mura, 1993). Therefore, any polynomial applied strain can be exactly counterbalanced by polynomial eigenstrains in the equivalence equation. In contrast, the eigenstrains outside the inclusion, which vanish at infinity, involve functions of the type $x^a\, y^b\, z^c\, (\sqrt[2]{x^2 + y^2 + z^2})^n$ where $n \le -(a + b + c + 3)$, and such terms cannot be exactly counterbalanced by a truncated Taylor series. These "external" strains act as applied strains arising from the surrounding interacting inhomogeneities. Two quantities based on the amplitude of the stress discontinuities and of the self induced body forces, calculated from the left hand side of eq. (7), will be proposed here to assess the quality of the solution.

4.1. STRESS JUMP AT THE INTERFACE OF THE INHOMOGENEITIES

The strain field induced by a stress free strain $\beta_j^p(a, b, c)$ in a domain Ω_p is continuous across the interface with another domain Ω_q. The approximate solution follows the stress gradients as well as possible by means of terms varying with a Taylor expansion around the centre r_q of Ω_q, i. e., a sum of terms $x^{a'}\, y^{b'}\, z^{c'}$. Although all terms are then correctly counterbalanced at the centre of an inhomogeneity, stress discontinuities σ_i^{dis} are expected to appear at the interface:

$$\sigma_i^{dis} = \sigma_i^{+} - \sigma_i^{-} \tag{10}$$

where $\boldsymbol{\sigma}_i^{+}$ and $\boldsymbol{\sigma}_i^{-}$ denote the components of the stress tensor at the external and internal faces respectively, corresponding to the left hand side of eq.(7). These discontinuities clearly increase as the distances between inhomogeneities decrease and as the difference between the material elastic constants ($\mathbf{C^p} - \mathbf{C}$) increases. Therefore, a quantity J_q derived from the stress discontinuities provides an estimate of the quality of the approximate solution. At the interface of a given inhomogeneity q, we propose to use a positive mean value based on the amplitude of the stress discontinuity. Since σ_i^{dis} increases with $C_{ij}^p - C_{ij}^0$, the displacement vector is employed as a normalization weight. Denoting by $\mathbf{u_q}$ the displacement vector at the centre of the inhomogeneity q of radius a_q, J_q is defined by:

$$J_q = \frac{3}{4\,\pi\, a_q^3\, (\boldsymbol{\varepsilon}^0 : \boldsymbol{\sigma}^0)} \int_{S_q} \left| (\boldsymbol{\sigma}^{dis}.\mathbf{n}) \right| . \left| (\mathbf{u} - \mathbf{u_q}) \right| \, ds \tag{11}$$

where $\mathbf{n}$ is the normal vector outward the interface and S_q is the surface of Ω_q. J_q is a dimensionless quantity, which is always positive and zero for the exact solution.

4.2. EQUILIBRIUM EQUATIONS INSIDE THE INHOMOGENEITIES

Outside the inclusions, as the elastic field is the sum of exact solutions and the remote field, the equilibrium equations are automatically satisfied for the right hand side of eq. (7). Using truncated series, the equilibrium equations inside an inhomogeneity give:

$$\mathrm{div} \left\{ \sum_{a', b', c'}^{0 \le a'+b'+c' \le T} \mathbf{C^p} \Big(\boldsymbol{\varepsilon}^{\mathbf{0p}}(a, b, c)(\mathbf{x}) + \sum_{q = 1}^{N} \mathsf{D}^{\mathbf{q}}(a', b', c')(\mathbf{x})\ \mathsf{B}^{\mathbf{q}}(a', b', c')(\mathbf{x}) \Big) \right\}$$

$$\approx \operatorname{div}\left\{ \sum_{a',b',c'}^{0 \le a'+b'+c' \le T} \mathbf{C}^0 \Big(\overset{0p}{\boldsymbol{\varepsilon}}(a,b,c)(\mathbf{x}) + \sum_{q=1}^{N} \overset{q}{\mathsf{D}}(a',b',c')(\mathbf{x})\ \overset{q}{\mathsf{B}}(a',b',c')(\mathbf{x}) - \overset{p}{\mathsf{B}}(a,b,c)(\mathbf{x}) \Big) \right\}$$

$$= 0 \qquad (12)$$

where the last term, a superposition of analytical solutions, is still zero. In fact, the fields arising from other inhomogeneities or from the inhomogeneity in question are free of body force. The parasitic body forces may be expected to tend to zero as the maximum order T of the Taylor series increases. Assuming that the strain applied at infinity is exactly described by a finite and small number of terms (< T), so that as in section 4.1 only the strain induced by the presence of neighbouring inhomogeneities must be described by an infinite number of terms, the parasitic body forces are expected to be proportional to the derivative of $\mathsf{D}^{\mathbf{q}}\ \mathsf{B}^{\mathbf{q}}$. Consequently, it remains to estimate the order of magnitude of the residual parasitic body forces f_i. In order to avoid a time consuming volume integration, the resultant **F** of **f** over the domain Ω_q is integrated over the internal surface S_q of the interface. $|\mathbf{F}|\ / S_q$ is expected to vary with the magnitude of $\boldsymbol{\sigma}^{dis}$. **F** increases with the coefficients of the stiffness tensor of the inhomogeneity and its amplitude may be used to estimate the quality of the solution. Nevertheless, due to the symmetric and antisymmetric nature of the strain distributions, some parasitic body forces can be hidden in cases of perfect symmetry. In such cases, one needs to integrate the resulting forces over six half spheres defined by the three planes (x = 0, y = 0, z = 0), but this is more time consuming. Since future applications will generally involve a random spatial distribution of inhomogeneities, we therefore propose a dimensionless quantity L_q as a measure of the level of accuracy to which the equilibrium equations are fulfilled within the domain Ω_q. L_q is obtained in the same manner as J_q by integrating eq. (12) over the surface S_q. Once again, a displacement vector related to $\mathbf{C}^{\mathbf{p}} - \mathbf{C}^{\mathbf{0}}$ is used as a normalization weight for **f**. L_q is then defined by:

$$L_q = \frac{3}{4\,\pi\, a_q^3\, (\boldsymbol{\varepsilon}^0 : \boldsymbol{\sigma}^0)} \left| \int_{S_q} (\boldsymbol{\sigma}^- .\mathbf{n})\, ds \right| . \left| \int_{S_q} (\mathbf{u} - \mathbf{u_q})\, ds \right| \qquad (13)$$

where the value of σ^- inside Ω_q may be calculated from the left hand side of eq. (7), using the solution obtained by solving eq. (9). L_q is obviously zero for cavities and this is also true for isotropic materials containing inhomogeneities with the same Poisson's ratio as the matrix. In the case of rubber like inhomogeneities, which behave approximately as a compressible fluid, L_q is likewise expected to be small.

5. ACCURACY OF THE METHOD

5.1. COMPARISON WITH RESULTS FROM THE LITERATURE: CASE OF CAVITIES

There exist only a few analytical reports relative to mechanical interactions between several spherical elastic inhomogeneities. The accuracy of the EIM, for a given truncation order T, may be expected to decay as the difference between the material constants of the inhomogeneities and the matrix increases. We consider here the case of two interacting identical spherical cavities of radius a (Rodin and Hwang, 1991; Sternberg and Sadowsky, 1952; Riccardi, 1998) under triaxial or uniaxial tension. Table I shows the ability of the EIM to estimate the stress concentration factors for remote equal triaxial tension. At separation distances d (Fig. 3) of less than 2.25 a, the errors in these factors are −12% and −19% for the third and second order computations, respectively. High stress gradients are in fact not correctly described in such cases, even by third order polynomials. In regions where no severe stress concentrations occur, the stresses are however correctly predicted, while the overall tendency of the EIM is to smooth the stress field. Table II gives results for uniaxial tension. Here it can be seen that the EIM tends to minimize the stress concentrations at all points on the interface, despite a good estimation at point A. As expected, the quality indicator J_q diminishes with increasing last order term T of the Taylor series and with decreasing stress concentration. Figure 4 shows the dependence of J_q on d / a for uniaxial and triaxial tension, the intersections of the curves for d / a < 2.01 being undoubtedly due to numerical integration. The quantity L_q (eq. 13) has no meaning for cavities. Finally, the EIM provides a good estimate (Appendix 1) of the energy release (Table III), which represents a mean value over the domain Ω_q.

d / a	σ_{xx} at point A		σ_{xx} at point B		σ_{zz} at point C	
	{exact} F.E.M.1 (F.E.M.2)	Present analysis (order m)	{exact} F.E.M.1	Present analysis (order m)	{exact} F.E.M.1	Present analysis (order m)
2.010	{7.51} 7.51 (7.36)	2.997 (3) 2.787 (2) 2.523 (1) 2.212 (0)	{1.54} 1.54	1.462 (3) 1.628 (2) 1.444 (1) 1.634 (0)	{1.43} 1.43	1.393 (3) 1.411 (2) 1.356 (1) 1.332 (0)
2.100	{3.16} 3.15 (3.10)	2.545 (3) 2.421 (2) 2.253 (1) 2.039 (0)	{1.54} 1.53	1.483 (3) 1.607 (2) 1.456 (1) 1.620 (0)	{1.43} 1.43	1.410 (3) 1.421 (2) 1.366 (1) 1.347 (0)
2.250	{2.35} 2.34 (2.30)	2.177 (3) 2.106 (2) 2.002 (1) 1.865 (0)	{1.53} 1.53	1.499 (3) 1.583 (2) 1.470 (1) 1.600 (0)	{1.43} 1.44	1.423 (3) 1.432 (2) 1.382 (1) 1.369 (0)
3.000	{1.71} 1.71 (1.73)	1.695 (3) 1.677 (2) 1.646 (1) 1.601 (0)	{1.52} 1.51	1.513 (3) 1.532 (2) 1.499 (1) 1.546 (0)	{1.45} 1.46	1.456 (3) 1.456 (2) 1.436 (1) 1.433 (0)
∞	–	1.500	–	1.500	–	1.500

Table I. Two interacting cavities (Fig. 3). Comparison of the stress concentration factors at points A, B and C estimated by the EIM (present analysis) and the FEM (F.E.M.1 and according to Rodin and Hwang (1991) F.E.M.2 in brackets) with the exact solution (Riccardi, 1998), for remote equal triaxial tension $\sigma_{xx} = \sigma_{yy} = \sigma_{zz} = 1$, $\mu^0 / K^0 = 0.6$.

All results were compared with the predictions of an elastic finite element analysis in order to check the validity of a finite element mesh for further elastic plastic calculations. The software CASTEM2000 allows automatic meshing of predefined surfaces and the computations involve axisymmetric irregular meshes. In cavity problems, the matrix consists of eight node quadrilateral elements and the dimensions of the domain are 6a x 8a in all cases. The boundaries remain straight and parallel while boundary displacements are imposed such that the mean strain corresponds to $\boldsymbol{\varepsilon}^0$. Since the solutions were compared to those for an infinite medium, the "remote" stress field was evaluated at the boundaries and the mean values between displacement and stress boundary conditions were used to normalize the results. Comparison with data from analytical calculations (Riccardi, 1998) and another recent FEM calculation (Rodin and Hwang, 1991) confirmed the validity of the mesh for all separation distances and justified its use for other kinds of inhomogeneities.

d / a	σ_{xx} at point A		σ_{xx} at point B		σ_{zz} at point C	
	{exact} F.E.M.1 (F.E.M.2)	Present analysis (order m)	{exact} F.E.M.1	Present analysis (order m)	{exact} F.E.M.1	Present analysis (order m)
2.010	{-0.778} -0.761 (-0.812)	-0.1514 (3) -0.1723 (2) -0.3987 (1) -0.8256 (0)	{-0.564} -0.559	-0.5413 (3) -0.5225 (2) -0.6925 (1) -0.4168 (0)	{1.85} 1.85	1.895 (3) 1.902 (2) 1.725 (1) 1.681 (0)
2.100	{-0.310} 0.302 (-0.320)	-0.1478 (3) -0.1824 (2) -0.3540 (1) -0.6640 (0)	{-0.564} -0.561	-0.5574 (3) -0.5168 (2) -0.6836 (1) -0.4292 (0)	{1.86} 1.86	1.903 (3) 1.910 (2) 1.740 (1) 1.703 (0)
2.250	{-0.208} -0.203 (-0.214)	-0.1382 (3) -0.1859 (2) -0.3201 (1) -0.5380 (0)	{-0.564} -0.562	-0.5728 (3) -0.5152 (2) -0.6682 (1) -0.4482 (0)	{1.87} 1.87	1.912 (3) 1.918 (2) 1.765(1) 1.737 (0)
3.000	{-0.288} -0.284 (-0.319)	-0.3079 (3) -0.3408 (2) -0.4047 (1) -0.4962 (0)	{-0.568} -0.565	-0.5782 (3) -0.5448 (2) -0.6120 (1) -0.5132 (0)	{1.91} 1.92	1.930 (3) 1.931 (2) 1.866 (1) 1.860 (0)
∞	–	-0.587	–	-0.587	–	2.022

Table II. Two interacting cavities (Fig. 3). Comparison of the stress concentration factors at points A, B and C estimated by the EIM (present analysis) and the FEM (F.E.M.1 and according to Rodin and Hwang (1991) F.E.M.2 in brackets) with the exact solution (Riccardi, 1998), for remote uniaxial tension $\sigma_{zz} = 1$, $\mu^0 / K^0 = 0.6$.

5.2. CASE OF GLASS PARTICLES IN A POLYMER MATRIX

The case of glass particles in an amorphous polymer matrix leads to morphologies similar to those of rubber toughened polymers. The ratio of the Young moduli of glass and polymer is 25, the Poisson ratios are respectively 0.23 and 0.4, and an analysis of the stresses for two interacting glass inhomogeneities is shown in Figure 5. It is seen that the EIM does not reach convergence, at least when the expansions are limited to an order of less than 4 and for a separation distance of less than 0.2 times the radius of the inhomogeneities. J_q values clearly indicate that a strong stress discontinuity arises at the interface as the inhomogeneities are located closer to one another. L_q values, related to the global equilibrium of an inhomogeneity, also indicate non convergence before the fourth order. The difference between the Poisson ratios leads to high values of L_q for zero order computations due to superposition of the fields attached to the outside of an inhomogeneity, which are in equilibrium only for a Poisson ratio equal to that of the matrix. Other calculations not presented here revealed that the harder the inhomogeneities, the poorer are the results given by the EIM.

	Triaxial tension $\sigma_{xx} = \sigma_{yy} = \sigma_{zz} = 1$				Uniaxial tension $\sigma_{zz} = 1$			
d / a	F.E.M.	Analytical	Present analysis, third order (J_q)		F.E.M.	Analytical	Present analysis, third order (J_q)	
2.001	-7.20	-7.17	-7.269	($1.14\ 10^{-1}$)	-3.51	-3.36	-3.478	($5.03\ 10^{-2}$)
2.010	-7.20	-7.17	-7.262	($1.08\ 10^{-1}$)	-3.52	-3.36	-3.482	($4.91\ 10^{-2}$)
2.050	-7.20	-7.16	-7.237	($8.57\ 10^{-2}$)	-3.55	-3.38	-3.500	($4.49\ 10^{-2}$)
2.100	-7.17	-7.16	-7.211	($6.51\ 10^{-2}$)	-3.58	-3.41	-3.522	($4.16\ 10^{-2}$)
2.250	-7.13	-7.12	-7.158	($3.08\ 10^{-2}$)	-3.65	-3.50	-3.585	($3.97\ 10^{-2}$)
2.500	-7.09	-7.10	-7.113	($1.21\ 10^{-2}$)	-3.75	? -3.77 ?	-3.679	($3.48\ 10^{-2}$)
3.000	-7.07	-7.08	-7.082	($4.23\ 10^{-3}$)	-3.91	-3.82	-3.834	($1.89\ 10^{-2}$)
4.000	-7.07	-	-7.070	($7.20\ 10^{-4}$)	-	-	-4.015	($3.81\ 10^{-3}$)
∞	-7.07	-7.07	-7.069	(0)	-4.20	-4.20	-4.200	(0)

Table III. Two interacting cavities (Fig. 3). Potential energy release per inhomogeneity for remote uniaxial or equal triaxial tension, $\mu^0 / K^0 = 0.6$. Comparison of results given by the EIM (third order) and the FEM (Rodin and Hwang, 1991) with the analytical solution.

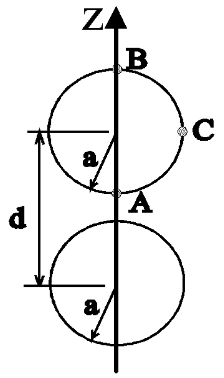

Figure 3. Two interacting spherical inhomogeneities in an infinite matrix. Positions of the points A, B and C at which the stress concentrations are computed, with the line AB defining the z-axis.

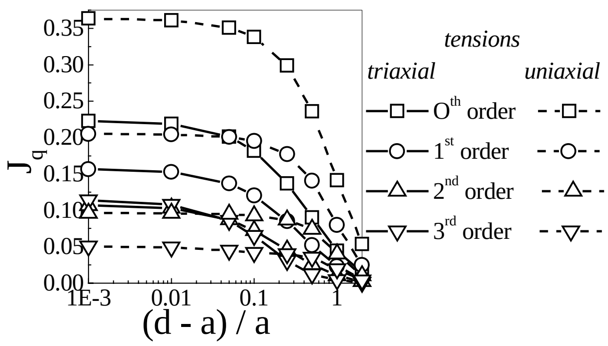

Figure 4. Stress discontinuities J_q for two interacting spherical cavities in an elastic matrix of Poisson's ratio 0.25 under remote triaxial or uniaxial tension.

6. ANALYSIS OF STRESSES FOR RUBBER INHOMOGENEITIES

The whitening of many polymeric materials is due to cavitation in a rubber phase, which is directly related to the magnitude of the positive (tensile) hydrostatic stress inside the rubber. Cavitation has a low energy consumption but plays the key role of initiating void growth and the subsequent plastic deformation and volume change. This process is relevant to the rubber toughening of amorphous materials such as polymethylmethacrylate (PMMA) and polystyrene (PS). Crack tip stress fields are associated with tensile states intermediate between triaxial and biaxial tension (plane strain or stress), depending on the thickness of the sample, whereas the classical tensile tests concern uniaxial tension. The following section examines the stress concentrations and hydrostatic stress for two interacting rubber inhomogeneities with axisymmetric geometry (Fig. 3), under triaxial, biaxial or uniaxial tension (Figs. 6, 7 and 8). The hydrostatic stress is well estimated by the EIM in all cases. Differences between the hydrostatic stress calculated at the centre of a rubber inhomogeneity and the mean hydrostatic stress calculated at the interface are always less than 0.17 %. A slight discrepancy for the FEM at large values of the interparticle distance d / a is undoubtedly due to the finite nature of the volume for this analysis, and in these cases the results of the EIM may in fact be considered to be more accurate than those of the FEM. The hydrostatic stress is more sensitive to the particle interaction under biaxial or uniaxial tension than under triaxial tension, while as expected a shielding effect is present for uniaxial tension (Fig. 8). The maximal von Mises stress concentrations (σ_e) are plotted with respect to the interparticle distance in Figure 9. In the case of triaxial tension, the maximum is always located at point A. The maximum for biaxial tension ranges from about point C to point A for values of d / a smaller than approximately 2.1, while for uniaxial tension this maximum lies at approximately point C for all values of d / a.

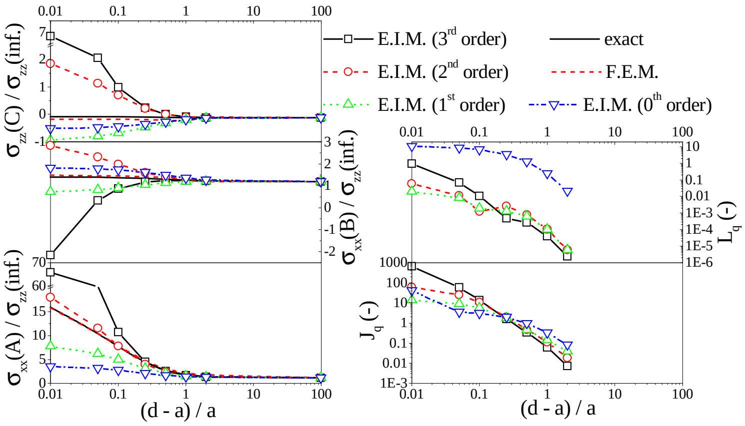

Figure 5. Two interacting glass inhomogeneities in a polymer matrix (Fig. 3). Comparison of the stress concentration factors at points A and C estimated by the EIM and the FEM with the exact solution (Riccardi, 1998), for remote uniaxial tension $\sigma_{zz} = 1$, $\mu^0 / K^0 = 0.2142$, $\mu^p / K^0 = 6.097$, $K^p / K^0 = 9.257$.

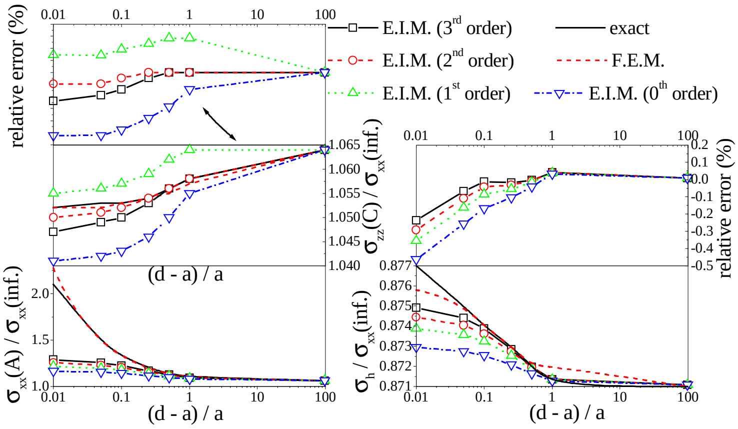

Figure 6. Two interacting rubber inhomogeneities in a polymer matrix (Fig. 3). Comparison of the stress concentration factors at points A and C and the hydrostatic stress in the rubber, σ_h, estimated by the EIM and the FEM with the exact solution (Riccardi, 1998), for remote equal triaxial tension $\sigma_{xx} = \sigma_{yy} = \sigma_{zz} = 1$, $\mu^0 / K^0 = 0.2142$, $\mu^p / K^0 = 2.097\ 10^{-4}$, $K^p / K^0 = 0.6$.

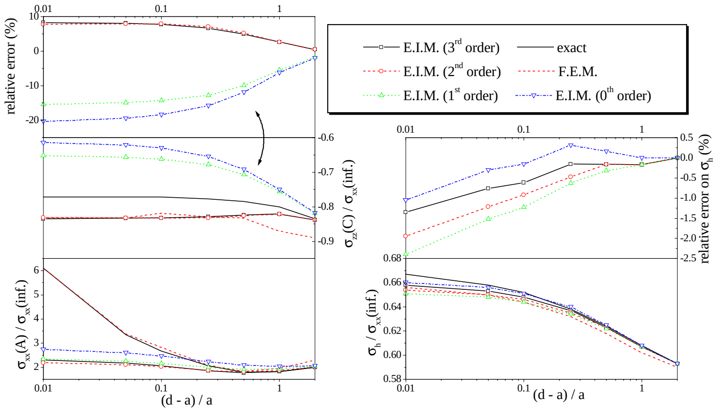

Figure 7. Two interacting rubber inhomogeneities in a polymer matrix (Fig. 3). Comparison of the stress concentration factors at points A and C and the hydrostatic stress in the rubber, σ_h, estimated by the EIM and the FEM with the exact solution (Riccardi, 1998), for remote equal biaxial tension $\sigma_{xx} = \sigma_{yy} = 1$, $\mu^0 / K^0 = 0.2142$, $\mu^p / K^0 = 2.097\ 10^{-4}$, $K^p / K^0 = 0.6$.

As in the case of stiff inhomogeneities, it is possible to find specific geometrical configurations for which convergence does not occur, at least before the fourth order. Considering the simple case of three identical rubber inhomogeneities located at the vertices of an equilateral triangle, in a plane inclined by 45° with respect to the axis of uniaxial tension and at a separation distance d = 0.1 *a, the J_q values increase by approximately 40 % at each successive order of expansion. This example illustrates the non systematic convergence of the EIM before the fourth order of Taylor series. Nevertheless, the level of hydrostatic stress does not vary significantly in this case with the order of expansion, only by less than 6.5 %.

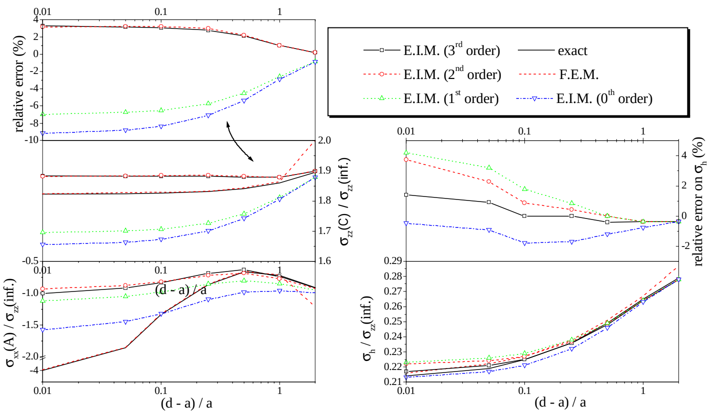

Figure 8. Two interacting rubber inhomogeneities in a polymer matrix (Fig. 3). Comparison of the stress concentration factors at points A and C and the hydrostatic stress in the rubber, σ_h, estimated by the EIM and the FEM with the exact solution (Riccardi, 1998), for remote uniaxial tension $\sigma_{zz} = 1$, $\mu^0 / K^0 = 0.2142$, $\mu^p / K^0 = 2.097\ 10^{-4}$, $K^p / K^0 = 0.6$.

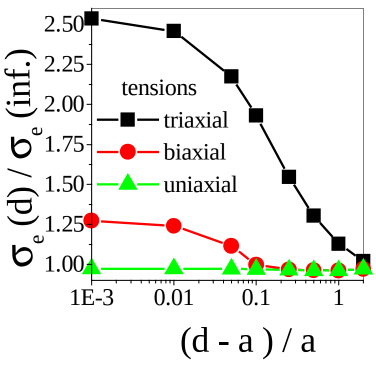

Figure 9. Two interacting rubber inhomogeneities in a polymer matrix (Fig. 3). Comparison of the evolution of the maximal von Mises stress with the separation distance for triaxial (σ_e = 0.199 σ_{xx} for d / a = ∞), biaxial (σ_e = 1.66 σ_{xx} for d / a = ∞) and uniaxial (σ_e = 1.74 σ_{zz} for d / a = ∞) tension. $\mu^0 / K^0 = 0.2142$, $\mu^p / K^0 = 2.097\ 10^{-4}$, $K^p / K^0 = 0.6$.

7. DISCUSSION

The EIM gives reasonably accurate results for the particular case of interacting cavities, where the stress concentration factors are well predicted provided that the separation distances exceed typically 10 % of the radius of the cavities. Parameters involving mean values over the volume of an inhomogeneity are likewise accurately estimated by the EIM for both cavities and rubber inhomogeneities. On the other hand, for inhomogeneities stiffer than the matrix, the discrepancy between the exact results and those of the EIM is large. This is clearly due to the high level of stress induced in a stiff neighbouring inhomogeneity by superposition of the elastic fields obtained for a single inhomogeneity in an infinite matrix. The quantities J_q and L_q, based respectively on stress discontinuities at the interface and static equilibrium, are therefore well suited to evaluate the accuracy of the EIM solutions for both soft and stiff inhomogeneities.

There are two reasons for the problems of convergence when third order expansions are used. Firstly, the functions involved in D are not well described by Taylor series outside the inclusions. Secondly, the $\beta_j^p(a, b, c)$ values obtained for an order of expansion of less than T $(a + b + c < T)$ depend on T. This could moreover explain some "instability" of the convergence, despite the impossibility of proving convergence or non convergence mathematically.

Although the EIM gives only approximate stress concentrations for realistic materials containing 10 % or more rubber, it seems to represent a good compromise between the required accuracy and the necessity of dealing with large numbers of particles in order to analyse the hydrostatic stress in rubber inhomogeneities (Géhant, 1999). Thus, rubber may be considered to behave to a first approximation as a compressible fluid. The order of magnitude of the variation of the hydrostatic stress in rubber inhomogeneities is then given by the ratio μ^p / K^p and the hydrostatic pressure is almost uniform and directly related to the volume change integrated over the entire volume of a particle. Consequently, zero order computations give accurate results for the hydrostatic stresses in rubber inhomogeneities.

The effect of interactions on stress concentrations is generally strong and may be expected to influence the occurrence of plasticity. In the case of uniaxial tension, the geometrical configuration used here induces a shielding effect and hence the influence of the separation distance on the von Mises stress concentration is almost zero. However, this influence increases with triaxiality and an amplifying effect is observed. Since the crack tip stress fields for thick plates are described by the results for remote equal triaxial tension, interactions are expected to strongly affect the occurrence of plasticity ahead of a crack tip. This remark is nevertheless obviously not valid in the case of invading plasticity.

8. CONCLUSIONS

As far as we know, there exists no ideal method of calculating the stresses induced by many interacting inhomogeneities. In the case of rubber-like inhomogeneities, where the parameter of interest is the hydrostatic stress inside an inhomogeneity, the EIM nevertheless gives reasonably accurate results, even for zero order expansions. This suggests that the EIM could be used to estimate the hydrostatic stress distributions in representative volume elements of rubber toughened PMMA or PS. However, it is still necessary to find a better way of combining the elementary eigenstrains, in order to check convergence of the method before the fourth order expansion of the Taylor series.

Acknowledgement. *The authors thank Dr P. Gilormini and Dr P. Suquet for helpful discussions.*

REFERENCES

Béguelin Ph., Approche Expérimentale du Comportement Mécanique des Polymères en Sollicitation Rapide, Ph. D. Thesis, (1996), 1572, Ecole Polytechnique Fédérale de Lausanne.

Chen H. S. and Acrivos A., The solution of the equations of linear elasticity for an infinite region containing two spherical inclusions, Int. J. Solids Structures, **14** (1978), 331-348.

Cherkaoui M., Sabar H. and Berveiller M., Elastic Composites with Coated Reinforcements: a Michromechanical Approach for Nonhomothetic Topology, Int. J. Engng. Sci., 33 (1995), 6, 829-843.

Dyson F. W., The Potentials of Ellipsoids of Variable Densities, Quarterly J. of Pure and Appl. Math., **25**, (1891), 259-288.

Eshelby J. D., The Determination of the Elastic Field of an Ellipsoidal Inclusion, and Related Problems, Proc. Roy. Soc. Lond. A, **241**, (1957), 376-396.

Eshelby J. D., The Elastic Field Outside an Ellipsoidal Inclusion, Proc. Roy. Soc. Lond. A, **252**, (1959), 561-569.

Ferrers N. M., On the Potentials of Ellipsoids, Ellipsoidal Shells, Elliptic Laminæ, and Elliptic Rings of Variable Densities, Quarterly J. of Pure and Appl. Math., **14**, (1877), 1-22.

Fond C., Mendels D., Ferrers J.-B.,. Kausch H. H and Hilborn J. G., Influence of Voids on the Stress Distribution and Deformation Behaviour of Epoxies under Uniaxial Deformation, J. Mat. Sc., **33**, (1998), 3975-3984.

Fond C., Lobbrecht A. and Schirrer R., Polymers toughened with rubber microspheres; an analytical solution for stresses and strains in the rubber particles at equilibrium and rupture, Int. J. Fract., **77**, (1996), 141-159.

Géhant S., Fond C. and Schirrer R., Damage in Rubber-Toughened Polymers : Micromechanical Simulations of Cavitation Involving Interactions Between Randomly Distributed Rubber Particles, Euromech 402, Micromechanics of Fracture Processes, 25-27 October, 1999, Seeheim, Germany.

Hill R. , New derivations of Some elastic Extremum Principles, Progress in Applied Mechanics - The Prager 60th Anniversary Volume, Macmillan, New York, (1963), 99-106.

Hort W. and Johnson W. C., Diffusional Boundary Conditions during Coarsening of Elastically Interacting Precipitates, Metallurgical and Materials Trans. A, **25**; (1994), 2695-2703.

Papkovitch P. F., Solution générale des équations différentielles fondamentales d'élasticité, exprimées par trois fonctions harmoniques, C.R. Acad. Sci. Paris, **195**, (1932), 513-515.

Matsuo T. and Noda N.-A., Interaction of Two Elliptical Inclusions and Two Ellipsoidal Inclusions, Int. Conf. Mat. Mech., F0-6C (1997), 199-204.

Moschovidis Z. A. and Mura T., Two-Ellipsoidal Inhomogeneities by the Equivalent Inclusion Method, J. Appl. Mech., Trans. ASME, (1975), 847-852.

Moulinec H. and Suquet P., A Numerical Method for Computing the Overall Response of Nonlinear Composites with Complex Microstructures, Comput. Methods Appl. Mech. Eng., **157**, (1998), 69-94.

Mura T., Micromechanics of Defects in Solids, Kluwer Academic Publishers, Dordrecht/Boston/London, (1993), second, revised edition, reprinted.

Neuber H., Kerbspannungslehre, Ann Arbor Mi., (1944), J.W. Edwards.

Phang-Thien N. and Kim S., The Load Transfer Between Two Rigid Spherical Inclusions in an Elastic Medium, Z. Angew. Math. Phys., **45**, (1994), 177-201.

Riccardi A., Etude Théorique de Configurations Inclusionnaires Non Classiques en Elasticité Linéaire Isotrope, Ph. D. Thesis, Ecole Nationale Supérieure des Mines de Saint-Etienne, 199TD, (1998).

Rodin G. J. and Hwang Y. L., On the Problem of Linear Elasticity for an Infinite Region Containing a Finite Number of Non-Intersecting Spherical Inhomogeneities, Int. J. Solids Structures, **27**, 2, (1991), 145-159.

Sabar H., Buisson M. and Berveiller M., The Inhomogeneous and Plastic Inclusion Problem with Moving Boundary, Int. J. Plasticity, **7**, (1991), 759-779.

Schirrer R., Fond C. and Lobbrecht A., Volume change and light scattering during mechanical damage in PMMA (Polymethylmethacrylate) toughened with core shell rubber particles, J. Mat. Sc., **31**, (1996), 6409-6422.

Sternberg E. and Sadowsky M. A., On the axisymmetric problem of the theory of elasticity for an infinite region containing two spherical cavities, J. Appl. Mech., **19**, (1952), 19-27.

Suquet P., A Simplified Method for the Prediction of Homogenized Elastic Properties of Composites with a Periodic Structure, C.R. Acad. Sci. Paris, **311**, (1990), 769-774.

Wu Y. and Nakagaki M., An Elastoplastic Constitutive Modeling of Particle Dispersed Composite, Int. Conf. Mat. Mech., B0-2A, (1997), 57-62.

APPENDIX 1 : ELASTIC ENERGY

Contrary to the preceding sections, we use for clarity in this appendix the classical indices for stress and strain. It can be demonstrated from Eshelby (1957) that the so-called interaction energy takes the same form for one or more inhomogeneities in the case of an exact solution. We first decompose the strain field ε_{ij} into the sum of the remote field ε^0_{ij} and the effect of all the eigenstrains e_{ij} arising from inhomogeneities, the respective associated displacement fields being $\mathbf{u^0}$ and $\mathbf{u^e}$. To obtain the state 1, an external pressure **t*** is applied at the interfaces of the inhomogeneities such that this state is related to e_{ij}. If σ^+_{ij} and σ^-_{ij} denote respectively the stresses induced by e just outside and inside an interface**, t*** is expressed as:

$$t^*_i = (\sigma^-_{ij} - \sigma^+_{ij})\, n_j \qquad \text{(A1. 1)}$$

where n is the normal vector away from the interface. Owing to the equilibrium at the interface, for an exact solution

$$(\sigma^-_{ij} + C^p_{ijkl}\,\varepsilon^0_{kl})\, n_j + (\sigma^+_{ij} + C^0_{ijkl}\,\varepsilon^0_{kl})\,(-n_j) = 0 \qquad \text{(A1. 2)}$$

so that

$$t^*_i = -\,(C^p_{ijkl} - C^0_{ijkl})\,\varepsilon^0_{kl}\, n_j \qquad \text{(A1. 3)}$$

At this stage, the elastic potential energy is

$$W_1 = \frac{1}{2}\sum_{p=1}^{N}\int_{S_p} \mathbf{t^*}\,\mathbf{u^e}\, ds \qquad \text{(A1. 4)}$$

where N is the number of inhomogeneities and S_p the surface of the p^{th} inhomogeneity. To obtain the final state, one then has to superimpose the field ε^0_{ij} on the state 1, with the result that ε^0_{ij} now generates tractions opposing **t***. Deducing the energy from the work of external forces leads to

$$W_{total} = \frac{1}{2}\sum_{p=1}^{N}\left\{\int_{S_p} \mathbf{t^*}\,(\mathbf{u^0} + \mathbf{u^e})\, ds + \int_{S_{ext}} C^0_{ijkl}\,(\varepsilon^0_{kl} + 2\, e_{kl})\, n_j\, u^0_i\, ds\right\} \qquad \text{(A1. 5)}$$

in which the stress term associated with e_{ij} is a second order term relative to $\mathbf{u^e}$. The stresses induced by eigenstrains are assumed to vanish at the boundary while the term associated with $C^0_{ijkl} e_{kl}\, n_j\, u^0_i$ in eq. (A1. 5) is assumed to be zero. Hence displacement boundary conditions are defined which are related to $\mathbf{u^0}$ at infinity. Applying Gauss's theorem in eq. (A1. 5) and using eq. (A1. 2) gives

$$W_{total} = W_0 + \frac{1}{2}\sum_{p=1}^{N}\int_{\Omega_p} (C^0_{ijkl} - C^p_{ijkl})\,\varepsilon^0_{kl}\,(\varepsilon^0_{ij} + e_{ij})\, dv \qquad \text{(A1. 6)}$$

where W_0 is the elastic energy induced by ε^0_{kl} if the medium did not contain any inhomogeneity. Noting from eq. (9) that $C^0_{ijkl}\,\beta_{kl} = (C^0_{ijkl} - C^p_{ijkl})\,(\varepsilon^0_{kl} + e_{ij})$, one finally obtains the classical result

$$W_{total} = W_0 \pm \sum_{p=1}^{N} \frac{1}{2}\int_{\Omega_p} C^0_{ijkl}\,\varepsilon^0_{ij}\,\beta_{ij}\,dv = W_0 \pm \Delta U \qquad \text{(A1. 7)}$$

the positive or negative sign depending on the boundary conditions: positive for stress and negative for displacement boundary conditions. The integral in the second term is the supplementary elastic energy related to the presence of inhomogeneities (Eshelby, 1957). It should be noted that eq. (A1. 7) can also be derived using variational principles (Hill, 1963). In the case of a uniform remote field $\boldsymbol{\varepsilon}$, it follows that any odd term in the expansion of β_{kl} in a Taylor series has no effect on the supplementary elastic energy ΔU. Since $\mathbf{e}(\mathbf{x}) = -\mathbf{e}(-\mathbf{x})$, the supplementary work done by external forces is in fact zero for odd terms.

Equation (A1. 7) involves Taylor series integrated over a spherical domain whereas both ε^0_{ij} and β_{kl} are of the form $x^a\,y^b\,z^c$. Changing into spherical coordinates gives

$$x = r\cos(\theta)\sin(\varphi)\ ,\ y = r\sin(\theta)\sin(\varphi)\ ,\ z = r\cos(\varphi)\ ,$$

$$I_{a\,b\,c} = \int_{\varphi=0}^{\pi}\int_{\theta=0}^{2\pi}\int_{r=0}^{R} \{r\cos(\theta)\sin(\varphi)\}^a\ \{r\sin(\theta)\sin(\varphi)\}^b\ \{r\cos(\varphi)\}^c\ r^2\sin(\varphi)\,dr\,d\theta\,d\varphi \qquad \text{(A1. 8)}$$

Using the notation $M_{p,\,q} = \int_{t=0}^{\pi/2} \{\sin(t)\}^p\,\{\cos(t)\}^q\,dt$, and remarking that $M_{p,\,q} = \frac{p-1}{q+p} M_{p-2,\,q}$ if $p \geq 2$, $M_{1,\,q} = \frac{1}{1+p}$, $M_{0,\,q} = \frac{(q-1)(q-3)\ ...\ 5.\ 3.\ 1}{q\,(q-2)(q-4)\ ...\ 6.\ 4.\ 2}$ if q is even, $M_{0,\,q} = \frac{(q-2)(q-4)\ ...\ 6.\ 4.\ 2}{(q-1)(q-3)\ ...\ 5.\ 3.\ 1}$ if q is odd and $M_{0,\,0} = \pi/2$, one obtains

$$I_{a\,b\,c} = \frac{8\,R^{a+b+c+3}}{a+b+c+3}\,M_{a,\,b}\,M_{a+b+1,\,c} \text{ if a and b and c are even} \qquad \text{(A1. 9)}$$

and as expected for an antisymmetric function, $I_{a\,b\,c} = 0$ if a, b or c is odd.

- First case $a = b = 0$ and $c \geq 0$ is even $\qquad I_{0\,0\,c} = \frac{4\,\pi\,R^{c+3}}{(c+3)(c+1)}$
- Second case $a \neq 0$, $b \neq 0$ are even and $c = 0$ $\qquad I_{a\,b\,0} = \frac{8\,R^{a+b+3}\ F(a)\,F(b)}{F(a+b+4)}$
- Third case $a \neq 0$, $b \neq 0$, $c \neq 0$ and all are even $\qquad I_{a\,b\,c} = \frac{8\,R^{a+b+c+3}\ F(a)\,F(b)\,F(c)}{F(a+b+c+4)}$

where $F(n) = (n-1)(n-3) \ldots 5.\,3.\,1.$

In the case of a uniform remote field, third order calculations give

$$U = U^0 - \sum_{q=1}^{N} \frac{2\,\pi\, r_q^{\,3}}{3}\, C^0_{ijkl}\, \overset{q}{\underset{ij}{\varepsilon}}(0,\,0,\,0)\ \Big\{\overset{q}{\underset{kl}{\beta}}(0,\,0,\,0) + \frac{r_q^{\,2}}{5}\,\Big(\overset{q}{\underset{kl}{\beta}}(2,\,0,\,0) + \overset{q}{\underset{kl}{\beta}}(0,\,2,\,0) + \overset{q}{\underset{kl}{\beta}}(0,\,0,\,2)\Big)\Big\} \tag{A1. 10}$$

This result is analogous to that presented in the appendix of Rodin and Hwang (1991).

APPENDIX 2 : ELASTIC POTENTIALS

Considering the equation (7) given in § 3.2, all displacements and strains are known once the volume integral Φ is known:

$$\Phi\,(\mathbf{x},\,a,\,b,\,c) = \int_\Omega \frac{x'^a\, y'^b\, z'^c}{|\mathbf{x'} - \mathbf{x}|}\, d\mathbf{x'} \tag{A2. 1}$$

Following [Ferrers, 1877; Dyson, 1891], Ω being a spherical domain, one obtains Φ analytically. The potential has a different expression Φ_i inside and Φ_o outside the domain Ω. Denoting a the radius of the spherical domain Ω and $r = |\mathbf{x}|$, these potentials inside the domain are:

$\Phi_i\,(\mathbf{x}\,/\,a,\,0,\,0,\,0) = 2\,\pi\,(a^2 - r^2\,/\,3)$

$\Phi_i\,(\mathbf{x}\,/\,a,\,1,\,0,\,0) = 2\,\pi\,(a\,x\,/\,3 - r^2\,x\,/\,5\,a)$

$\Phi_i\,(\mathbf{x}\,/\,a,\,2,\,0,\,0) = \pi\,(a^2\,/\,3 - 2\,r^2\,/\,15 + r^4\,/\,35\,a^2 + 2\,x^2\,/\,5 - 2\,r^2\,x^2\,/\,7\,a^2)$

$\Phi_i\,(\mathbf{x}\,/\,a,\,1,\,1,\,0) = 2\,\pi\,(x\,y\,/\,5 - r^2\,x\,y\,/\,7\,a^2)$

$\Phi_i\,(\mathbf{x}\,/\,a,\,3,\,0,\,0) = \pi\,(a\,x\,/\,5 - 6\,r^2\,x\,/\,35\,a + r^4\,x\,/\,21\,a^3 + 2\,x^3\,/\,7\,a - 2\,r^2\,x^3\,/\,9\,a^2)$

$\Phi_i\,(\mathbf{x}\,/\,a,\,2,\,1,\,0) = \pi\,(a\,y\,/\,15 - 2\,r^2\,y\,/\,35\,a + r^4\,y\,/\,63\,a^3 + 2\,x^2\,y\,/\,7\,a - 2\,r^2\,x^2\,y\,/\,9\,a^3)$

$\Phi_i\,(\mathbf{x}\,/\,a,\,1,\,1,\,1) = \pi\,(2\,x\,y\,z\,/\,7\,a - 2\,r^2\,x\,y\,z\,/\,9\,a^3)$

$\Phi_i\,(\mathbf{x}\,/\,a,\,4,\,0,\,0) = \pi\,(2\,a^2\,/\,15 - 2\,r^2\,/\,35 + 2\,r^4\,/\,105\,a^2 - 2\,r^6\,/\,693\,a^4 + 6\,x^2\,/\,35 - 4\,r^2\,x^2\,/\,21\,a^2 + 2\,r^4\,x^2\,/\,33\,a^4 + 2\,x^4\,/\,9\,a^2 - 2\,r^2\,x^4\,/\,11\,a^4)$

$\Phi_i\,(\mathbf{x}\,/\,a,\,3,\,1,\,0) = \pi\,(3\,x\,y\,/\,35 - 2\,r^2\,x\,y\,/\,21\,a^2 + r^4\,x\,y\,/\,33\,a^4 + 2\,x^3\,y\,/\,9\,a^2 - 2\,r^2\,x^3\,y\,/\,11\,a^4)$

$\Phi_i\,(\mathbf{x}\,/\,a,\,2,\,2,\,0) = \pi\,(2\,a^2\,/\,45 - 2\,r^2\,/\,105 + 2\,r^4\,/\,315\,a^2 - 2\,r^6\,/\,2079\,a^4 + x^2\,/\,35 - 2\,r^2\,x^2\,/\,63\,a^2 + r^4\,x^2\,/\,99\,a^4 + y^2\,/\,35 - 2\,r^2\,y^2\,/\,63\,a^2 + r^4\,y^2\,/\,99\,a^4 + 2\,x^2\,y^2/\,9\,a^2 - 2\,r^2\,x^2\,y^2/\,11\,a^4)$

$\Phi_i\,(\mathbf{x}\,/\,a,\,2,\,1,\,1) = \pi\,(y\,z\,/\,35 - 2\,r^2\,y\,z\,/\,63\,a^2 - r^4\,y\,z\,/\,99\,a^4 + 2\,x^2\,y\,z\,/\,9\,a^2 - 2\,r^2\,x^2\,y\,z\,/\,11\,a^4)$

$\Phi_i\,(\mathbf{x}\,/\,a,\,5,\,0,\,0) = \pi\,(2\,a\,x\,/\,21 - 2\,r^2\,x\,/\,21\,a + 10\,r^4\,x\,/\,231\,a^3 - 10\,r^6\,x\,/\,1287\,a^5 + 10\,x^3\,/\,63\,a - 20\,r^2\,x^3\,/\,99\,a^3 + 10\,r^4\,x^3\,/\,143\,a^5 + 2\,x^5\,/\,11\,a^3 - 2\,r^2\,x^5\,/\,13\,a^5)$

$\Phi_i\,(\mathbf{x}\,/\,a,\,4,\,1,\,0) = \pi\,(2\,a\,y\,/\,105 - 2\,r^2\,y\,/\,105\,a + 2\,r^4\,y\,/\,231\,a^3 - 2\,r^6\,y\,/\,1287\,a^5 + 2\,x^2\,y\,/\,21\,a - 4\,r^2\,x^2\,y\,/\,33\,a^3 + 6\,r^4\,x^2\,y\,/\,143\,a^5 + 2\,x^4\,y\,/\,11\,a^3 - 2\,r^2\,x^4\,y\,/\,13\,a^5)$

$\Phi_i\,(\mathbf{x}\,/\,a,\,3,\,2,\,0) = \pi\,(2\,a\,x\,/\,105 - 2\,r^2\,x\,/\,105\,a + 2\,r^4\,x\,/\,231\,a^3 - 2\,r^6\,x\,/\,1287\,a^5 + x^3\,/\,63\,a - 2\,r^2\,x^3\,/\,99\,a^3 + r^4\,x^3\,/\,143\,a^5 + x\,y^2\,/\,21\,a - 2\,r^2\,x\,y^2\,/\,33\,a^3 + 3\,r^4\,x\,y^2\,/\,143\,a^5 + 2\,x^3\,y^2\,/\,11\,a^3 - 2\,r^2\,x^3\,y^2\,/\,13\,a^5)$

$\Phi_i\,(\mathbf{x}\,/\,a,\,3,\,1,\,1) = \pi\,(x\,y\,z\,/\,21\,a - 2\,r^2\,x\,y\,z\,/\,33\,a^3 + 3\,r^4\,x\,y\,z\,/\,143\,a^5 + 2\,x^3\,y\,z\,/\,11\,a^3 - 2\,r^2\,x^3\,y\,z\,/\,13\,a^5)$

$\Phi_i\,(\mathbf{x}\,/\,a,\,2,\,2,\,1) = \pi\,(2\,a\,z\,/\,315 - 2\,r^2\,z\,/\,315\,a + 2\,r^4\,z\,/\,693\,a^3 - 2\,r^6\,z\,/\,3861\,a^5 + x^2\,z\,/\,63\,a - 2\,r^2\,x^2\,z\,/\,99\,a^3 + r^4\,x^2\,z/\,143\,a^5 + y^2\,z\,/\,63\,a - 2\,r^2\,y^2\,z\,/\,99\,a^3 + r^4\,y^2\,z\,/\,143\,a^5 + 2\,x^2\,y^2\,z\,/\,11\,a^3 - 2\,r^2\,x^2\,y^2\,z\,/\,13\,a^5)$

(A2. 2)

and outside the domain are:

Φ_o (**x** / a, 0, 0, 0) = $4 \pi (a^3 / 3 r)$

Φ_o (**x** / a, 1, 0, 0) = $4 \pi (a^4 x / 15 r^3)$

Φ_o (**x** / a, 2, 0, 0) = $4 \pi (- a^5 / 105 r^3 + a^3 / 15 r + a^5 x^2 / 35 r^5)$

Φ_o (**x** / a, 1, 1, 0) = $4 \pi (x y a^5 / 35 r^5)$

Φ_o (**x** / a, 3, 0, 0) = $4 \pi (- a^6 x / 105 r^5 + a^4 x / 35 r^3 + a^6 x^3 / 63 r^7)$

Φ_o (**x** / a, 2, 1, 0) = $4 \pi (- a^6 y / 315 r^5 + a^4 y / 105 r^3 + a^6 x^2 y / 63 r^7)$

Φ_o (**x** / a, 1, 1, 1) = $4 \pi (a^6 x y z / 63 r^7)$

Φ_o (**x** / a, 4, 0, 0) = $4 \pi (- a^7 / 1155 r^5 - 2 a^5 / 315 r^3 + a^3 / 35 r - 2 a^7 x^2 / 231 r^7 + 2 a^5 x^2 / 105 r^5 + a^7 x^4 / 99 r^9)$

Φ_o (**x** / a, 3, 1, 0) = $4 \pi (- a^7 x y / 231 r^7 + a^5 x y / 105 r^5 + a^7 x^3 y / 99 r^9)$

Φ_o (**x** / a, 2, 2, 0) = $4 \pi (a^7 / 3465 r^5 - 2 a^5 / 945 r^3 + a^3 / 105 r - a^7 x^2 / 693 r^7 + a^5 x^2 / 315 r^5 - a^7 y^2 / 693 r^7 + a^5 y^2 / 315 r^5 + a^7 x^2 y^2 / 99 r^9)$

Φ_o (**x** / a, 2, 1, 1) = $4 \pi (- a^7 y z / 693 r^7 + a^5 y z / 315 r^5 + a^7 x^2 y z / 99 r^9)$

Φ_o (**x** / a, 5, 0, 0) = $4 \pi (5 a^8 x / 3003 r^7 - 2 a^6 x / 231 r^5 + a^4 x / 63 r^3 - 10 a^6 x^3 / 1287 r^9 + 10 a^6 x^3 / 693 r^7 + a^8 x^5 / 143 r^{11})$

Φ_o (**x** / a, 4, 1, 0) = $4 \pi (a^8 y / 3003 r^7 - 2 a^6 y / 1155 r^5 + a^4 y / 315 r^3 - 2 a^8 x^2 y / 429 r^9 + 2 a^6 x^2 y / 231 r^7 + a^8 x^4 y / 143 r^{11})$

Φ_o (**x** / a, 3, 2, 0) = $4 \pi (a^8 x / 3003 r^7 - 2 a^6 x / 1155 r^5 + a^4 x / 315 r^3 - a^8 x^3 / 1287 r^9 + a^6 x^3 / 693 r^7 - a^8 x y^2 / 429 r^9 + a^6 x y^2 / 231 r^7 + a^8 x^3 y^2 / 143 r^{11})$

Φ_o (**x** / a, 3, 1, 1) = $4 \pi (- a^8 x y z / 429 r^9 + a^6 x y z / 231 r^7 + a^8 x^3 y z / 143 r^{11})$

Φ_o (**x** / a, 2, 2, 1) = $4 \pi (a^8 z / 9009 r^7 - 2 a^6 z / 3465 r^5 + a^4 z / 945 r^3 - a^8 x^2 z / 1287 r^9 + a^6 x^2 z / 693 r^7 - a^8 y^2 z / 1287 r^9 + a^6 y^2 z / 693 r^7 + a^8 x^2 y^2 z / 143 r^{11})$

(A2. 3)